Journal of Inorganic and General Chemistry
ZAAC
Zeitschrift für anorganische und allgemeine Chemie
www.zaac.wiley-vch.de
RESEARCH ARTICLE

DOI: 10.1002/zaac.202300164

Special Collection

$K_7In_4As_6$ and K_3InAs_2 - Two more Zintl phases showing the rich variety of In-As polyanion structures

Marina Boyko,[a] Viktor Hlukhyy,[a] and Thomas F. Fässler*[a]

Dedicated to the late Professor Eduard Zintl on the occasion of his 125th birthday

Binary phases of triel (*Tr*) and pentel (*Pn*) elements (III-V semiconductors) represent a unique compound class due to their tunable intrinsic band gap in dependency of the element combination. We report here on two new compounds in the ternary system K–In–As. In K_3InAs_2 the edge-sharing tetrahedral $InAs_4$ units are connected via opposed edges of the tetrahedra forming linear $[InAs_2]^{3-}$ chains and are thus iso(valence)-electronic with SiS_2. In $K_7In_4As_6$, the $InAs_4$ tetrahedra are connected via neighboring edges of the tetrahedra forming zig-zag chains. These chains are linked in two directions through dimeric $[As_3In–InAs_3]$ units. Both reported Zintl phases extend the number of structures that possess the same In–As ratio. In K_3InAs_2 a one-dimensional polyanion in contrast to known Na_3InAs_2 comprising a three-dimensional polyanion structure is found. $K_7In_4As_6$ forms together with the known phases $K_2In_2As_3$ and $K_3In_2As_3$ a series of Zintl phases with the ratio In : As = 2 : 3. Even though the three phases differ only slightly in their valence electron concentration (VEC) of the polyanion, the VECs have a strong influence on the structures. Syntheses, crystal structures and the electronic band structures are reported. The compounds are discussed in the context of the Zintl concept.

Introduction

The elements of group 14 and the isoelectronic binary compounds comprising group 13 (*Tr*) and group 15 (*Pn*) elements attract much interest due to their semiconducting properties. They provide a variety of band gaps and properties that can be modified by extrinsic doping, temperature, pressure, etc.[1] Compounds such as GaAs are among the most important III–V semiconductors[2] and thus are important materials for the development of electronic devices e.g. in transistors or in light-emitting diodes on which our modern information age is based. As common building blocks, the binary semiconducting compounds possess linked tetrahedral triel pnictides $TrPn_4$.

In this work, our attention focuses on mixtures of group 13 and 15 elements, that are modified by alkali metals. In addition, a rich plethora of structures in combination with alkaline-earth metals has been reported.[3] A large number of compounds with alkali metals contain heteroatomic anions $[Tr_xPn_y]^{z-}$ with different compositions, charges and bonding situations. With the highest amount of alkali metals, isolated trigonal fragments $[TrPn_3]^{6-}$ such as $[InAs_3]^{6-}$[4] and associated dimers, trimers or condensed five-membered rings such as $[Ga_2P_4]^{6-}$,[5] $[Ga_3As_6]^{9-}$,[6] and $–[Ga_2As_3]–^{}$[7] occur on one hand, or discrete tetrahedral $[TrPn_4]^{9-}$ units[8] such as $[AlP_4]^{9-}$[8a] as well as related dimers, linear or two- and three-dimensional polymers occur on the other hand. Notice, that in case of the basic unit $[TrPn_3]^{6-}$ mesomeric forms with *Tr-Pn* double bonds support the planarity of the $[TrPn_3]$ unit, and such units are even found among the heavier homologues of the *Tr* and *Pn* elements such as Ga and Bi,[9] which is in contrast to the well-known 'double bond rule'.[10] The $[TrPn_3]$ units might be interconnected in different ways by sharing edges, faces, corners, to build up three dimensional structures. Recently, $K_{10}Ga_3Bi_{6.65}$ has been reported containing linked trimers of $[GaBi_3]$ units forming slightly deformed hexagonal $[Ga_3Bi_6]^{9-}$ polyanions with planar triangular-coordinated Ga by Bi atoms beside isolated Bi–Bi dumbbells.[9] Among these structures, the nature of the anionic framework is collectively related to the number, the size, and the charge of the cations and, in turn, to the atomic ratio and thus the charge of the $[Tr_xPn_y]^{z-}$ anion and its valence electron concentration. Consequently, with a smaller amount of alkali metal and thus *Tr-Pn* polyanions with lower charge of the general composition $[Tr_xPn_y]^{z-}$ exhibit one-, two- or three-dimensional anionic frameworks with decreasing alkali metal content.[11]

In the ternary *A* < C- > In–As systems six compounds have been reported to date (Figures 1 and S1, Supporting Information). Trigonal planar $[InAs_3]^{6-}$ anions (isostructural to BO_3^{3-} or CO_3^{2-}) with the highest alkali metal content are observed in

[a] *M. Boyko, V. Hlukhyy, T. F. Fässler*
Department Chemie, TUM School of Natural Sciences, Technische Universität München, Lichtenbergstr. 4, D-85747 Garching/Germany
E-mail: thomas.faessler@lrz.tum.de

Supporting information for this article is available on the WWW under https://doi.org/10.1002/zaac.202300164

This article is part of a Special Collection to celebrate Professor Eduard Zintl on the occasion of his 125th anniversary. Please see our homepage for more articles in the collection.

Journal of Inorganic and General Chemistry
ZAAC
Zeitschrift für anorganische und allgemeine Chemie

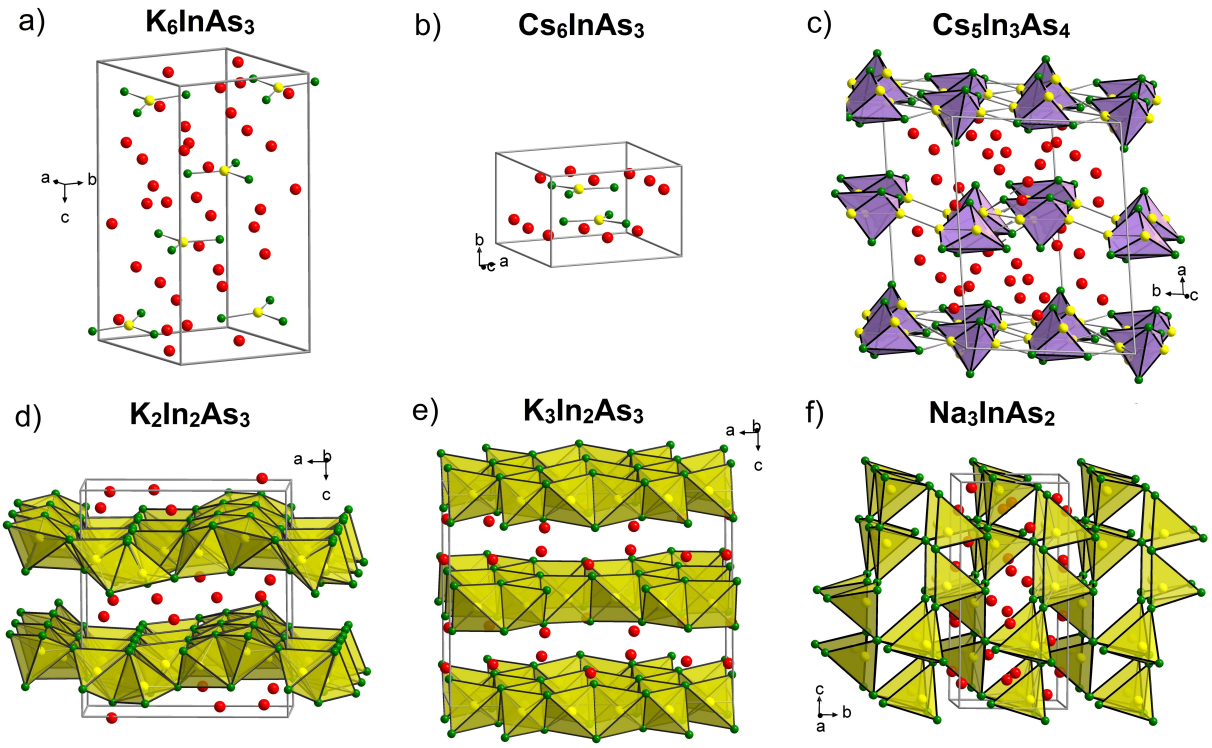

Figure 1. Structures of ternary *A*–In–As compounds (*A* = alkali metal). Trigonal planar $[InAs_3]^{6-}$ anions in the structures of compounds with stoichiometry 6:1:3 (a,b); layers of interconnected defect cubanes –$[In_3As_4]$– in the structure of $Cs_5In_3As_4$ (c); $[InAs_4]$ tetrahedra connected via common corners into two-dimensional nets in $K_2In_2As_3$ (d), $K_3In_2As_3$ (e), and the two-dimensional net in Na_3InAs_2 (f). *A* atoms are shown in red, In atoms in yellow and As atoms in green color.

K_6InAs_3[4b] and Cs_6InAs_3[4a] (Figure 1a,b). A quite unusual anionic substructure is found in $Cs_5In_3As_4$[12] (Figure 1c), which contains repeating structural units that can be describes as defect cubanes of three indium and four arsenic atoms, $[In_3As_4]$, that are interconnected via In–In and In–As bonds into chains and layers. The compound can be considered as made of two coexisting polymorphic forms built up by chains and layers. For the other compounds with layered structures, $InAs_4$ tetrahedra are connected by common edges, faces or corners. These layers are typically separated by *A* atoms. The most common structure type among *A*–*Tr*–*Pn* compounds is observed for a 2:2:3 stoichiometry ($Na_2Al_2Sb_3$-type), which is shown as an example for $K_2In_2As_3$ in Figure 1d.[13] This structure can be described as $InAs_4$ tetrahedra connected via common vertices to two-dimensional nets, comprising also tetrahedra connected via As–As bonds (Figure 1d). In $K_3In_2As_3$[14] edge sharing $InAs_4$ tetrahedra form four-membered and twelve-membered rings which are connected to layers (Figure 1e). Na_3InAs_2 with its smaller Na^+ cations has a polyanionic 3D structure with tetrahedrally coordinated In by As atoms (Figure 1f).[15] The special structural features in Na_3InAs_2 are channels formed by twelve-membered rings. All In atoms within the $[InAs_2]^{3-}$ polyanion are four-fold coordinated by As atoms, whereas the As atoms are two-fold bonded to In atoms.

Here we report on a novel ternary, electron-precise compounds with layered and one-dimensional polyanions of interconnected $InAs_4$ tetrahedra.

Experimental Section

Synthesis. $K_7In_4As_6$, was obtained, similar to the recently reported compound $K_{10}Ga_3Bi_{6.65}$,[9] first from the elements in a quaternary sample K, Cu, In and As with the ratio 1:1:0.9:1.5 (61.2 mg K, 99.4 mg Cu, 163.6 mg In and 175.8 mg As; sample 1). The aim of this synthesis was to obtain a compound, similar to $Na_{12}Cu_{12}Sn_{21}$, substituting Sn with a mixture of In and As. The elements were packed and sealed in a Nb ampoule using a modified Mini Arc Melting system (MAM-1, Johanna Otto GmbH) with a water-cooled copper-hearth in an argon filled Glovebox (MBraun 20G, argon purity 99.996%). Then the sample was enclosed in graphitized silica tubes and annealed in a muffle furnace. A two-stage temperature program was applied: the first stage was heating to 1073 K with a rate of 5 K/min and holding for 12 h, and the second stage was slow (0.1 K/min) cooling to 773 K and holding the temperature for 60 h.

The ampoule was opened in a glove box, and capillaries (Hilgenberg GmbH, 0.3 mm inner diameter) were prepared for powder X-ray diffraction analysis on Stoe StadiP diffractometers with Ge (111) monochromized Cu-$K_{\alpha1}$ (1.54056 Å) radiation. PXRD analysis using WinXPOW[16] revealed the formation of $K_7In_4As_6$ as the main product (Figure S2, Supporting Information). Therefore, the sample 2 with a K:In:As ratio of 7:4:6 was synthesized from

pure elements (115.7 mg of K, 194.2 mg of In and 190.1 mg of As) in a sealed niobium ampoule with the following temperature program: heating with 5 K/min to 873 K, holding the temperature for 200 h followed by quenching to room temperature. Phase analysis of the obtained sample measured on a Stoe StadiP diffractometer with Mo-$K_{\alpha1}$ (0.70930 Å) radiation showed the presence of two ternary phases: K_3InAs_2 and $K_7In_4As_6$ (Figure S3, Supporting Information).

Considering the toxicity of arsenic and its compounds, as well as their sensitivity to air, all manipulations were carried out in an argon filled glove box. All rests of the samples were properly disposed of according to the safety instructions. Welded Nb ampoules were additionally enclosed in a graphitized silica tube and heated in a muffle furnace placed in a fume hood. All samples showed high sensitivity toward air and moisture.

Structure Determination. Single crystals were picked from the reaction products (sample 1) in a glove box, and data collection was performed on a Stoe StadiVari diffractometer. Shiny block-shaped dark gray single crystals of $K_7In_4As_6$ were selected and measured at 150 K under a constant N_2 flow with a detector distance of 70 mm and an exposure time of 15 seconds. The unit cell was indexed in the triclinic space group $P\bar{1}$ with cell parameters $a=9.1098(3)$, $b=9.1641(4)$, $c=24.4564(9)$ Å, $\alpha=95.796(3)$, $\beta=92.578(3)$, $\gamma=90.013(3)$ °). The structure was solved by Direct Methods (SHELXS-2014) and refined by full-matrix least-squares calculations against F^2 (SHELXL-2014).[17] Data reduction and multi-scan absorption correction were carried out with the X-AREA (version 1.88, Stoe) and the STOE LANA (version 1.77.1, Stoe) software packages, respectively.[18] Crystallographic data and selected data and details of the structure refinement for $K_7In_4As_6$ are listed in Table 1. Atomic parameters and isotropic displacement parameters for all eight crystallographically independent indium, twelve arsenic and fourteen potassium atoms are listed in Table S1 (Supporting Information). Table S2 (Supporting Information) contains all interatomic distances in $K_7In_4As_6$. Energy dispersive X-ray (EDX) analysis of the measured crystal confirmed the presence of the three elements (Table S3, Supporting Information) in the ratio K:In:As of 38:26:36 (19:13:18).

K_3InAs_2 is isostructural to K_3InP_2,[19][20] thus the structure determination was straight-forward, and both structures reveal similarities. A shiny grey crystal was selected for the single crystal X-ray diffraction analysis from the sample 2 and measured on a Stoe StadiVari diffractometer at 150 K under a constant N_2 flow. The unit cell was indexed in the orthorhombic space group *Ibam* with cell parameters $a=7.821(2)$, $b=14.759(3)$ and $c=6.936(1)$ Å. Table 1 contains selected crystallographic data of the refinement of K_3InAs_2. Atomic parameters and isotropic displacement parameters are listed in Table S4 (Supporting Information). Interatomic distances are given in Table S5 (Supporting Information). In the structure of K_3InAs_2 four crystallographically independent positions are fully occupied by In (position 4*a*), As (8*j*) and two by K atoms (8*j* and 4*b*), resulting in four formula units per unit cell. EDX analysis (Table S6, Supporting Information) confirmed the presence of all three elements and the expected stoichiometry.

Further details of the crystal structure investigations may be obtained from the Cambridge Crystallographic Data Centre, CCDC, 12 Union Road, Cambridge CB21EZ, UK (Fax: +44-1223-336-033; E-mail: deposit@ccdc.cam.ac.uk) on quoting the depository numbers CSD-2267029 for $K_7In_4As_6$ and CSD-2267028 for K_3InAs_2.

Electronic Structure Calculations. The linear muffin-tin orbital (LMTO) method in the atomic sphere approximation (ASA) using the tight-binding (TB) program TB-LMTO-ASA[21] was employed to analyze the electronic structures of $K_7In_4As_6$ and K_3InAs_2. The radii of the muffin-tin spheres were determined after Jepsen and Andersen.[22] The following valence functions were used for the basis set for the short-ranged atom-centered TB-LMTOs: s-d valence functions for K, s-p valence functions for In and s, p valence functions for As. K 4p orbitals were treated by the downfolding technique.[23] The density of states (DOS) analysis has been done for partial and total DOS of $K_7In_4As_6$ and K_3InAs_2 including the iDOS.

The choice of the lattice vectors as the implemented path X-Γ-Y-Γ-Z-Γ-U-V and Γ-L-B-R-W-S-Γ-X-Γ-S-T-W for $K_7In_4As_6$ and K_3InAs_2, respectively, was selected as it was suggested in[24] for the triclinic Brillouin zone of TRI_{1b} and the orthorhombic Brillouin zone of the $ORCF_2$ lattice, respectively, using the Bilbao Crystallographic Server.[25]

Table 1. Crystallographic data and selected details of the structure refinement of $K_7In_4As_6$ and K_3InAs_2.

Formula	$K_7In_4As_6$	K_3InAs_2
Formula weight ($g\cdot mol^{-1}$)	1414.18	190.98
Space group	$P\bar{1}$ (no. 2)	*Ibam* (no. 72)
Z	4	4
Unit cell parameters (Å/°)	$a=9.1098(3)$ $b=9.1641(4)$ $c=24.4564(9)$ $\alpha=95.796(3)$ $\beta=92.578(3)$ $\gamma=90.013(3)$	$a=7.821(2)$ $b=14.759(3)$ $c=6.936(1)$
Volume ($Å^3$)	2029.2(1)	800.7(3)
$D_{calcd.}$ ($g\,cm^{-3}$)	3.87	3.17
Abs. Coeff. (mm^{-1})	15.6	12.6
F(000) (e)	2108	688
Crystal shape/color	block/dark grey	block/grey
Temperature (K)	150(2)	150(2)
Θ range (deg)	2.735–26.500	2.948–29.993
Range in *hkl*	$\pm11\pm11-29\div30$	$\pm10, \pm20, \pm9$
Reflections collected	27370 ($R_\sigma=0.0469$)	14688 ($R_\sigma=0.0254$)
Unique reflections	7043 ($R_{int}=0.0574$)	566 ($R_{int}=0.1015$)
Data/parameter	8427/308	628/ 19
GOF on F^2	1.035	1.014
R_1, wR_2 ($I>2\,\sigma(I)$)	0.0481, 0.1281	0.0315, 0.0794
R_1, wR_2 (*all data*)	0.0644, 0.1590	0.0355, 0.0770
Largest diff. peak/hole ($e\,Å^{-3}$)	2.656/−3.750	1.435/−1.562

Results

Crystal Structures. The crystal structure of $K_7In_4As_6$ is rather complex and isostructural to $Cs_7In_4Bi_6$.[26] It shows the typical tetrahedral coordination of the In atoms by four As atoms, similar to that in other ternary *A–Tr–Pn* systems. The polyanionic substructure of $K_7In_4As_6$ can be described as a chain of connected $InAs_4$ tetrahedra sharing two out of six edges of the tetrahedra (Figure 2a). The low symmetry is quite unusual and a result of different motifs of edge-sharing tetrahedra that cause twists and turns of the chains, which also result in a long *c* axis. The stacking of the In-centered tetrahedra within one layer from different perspectives is shown in Figure 2b.

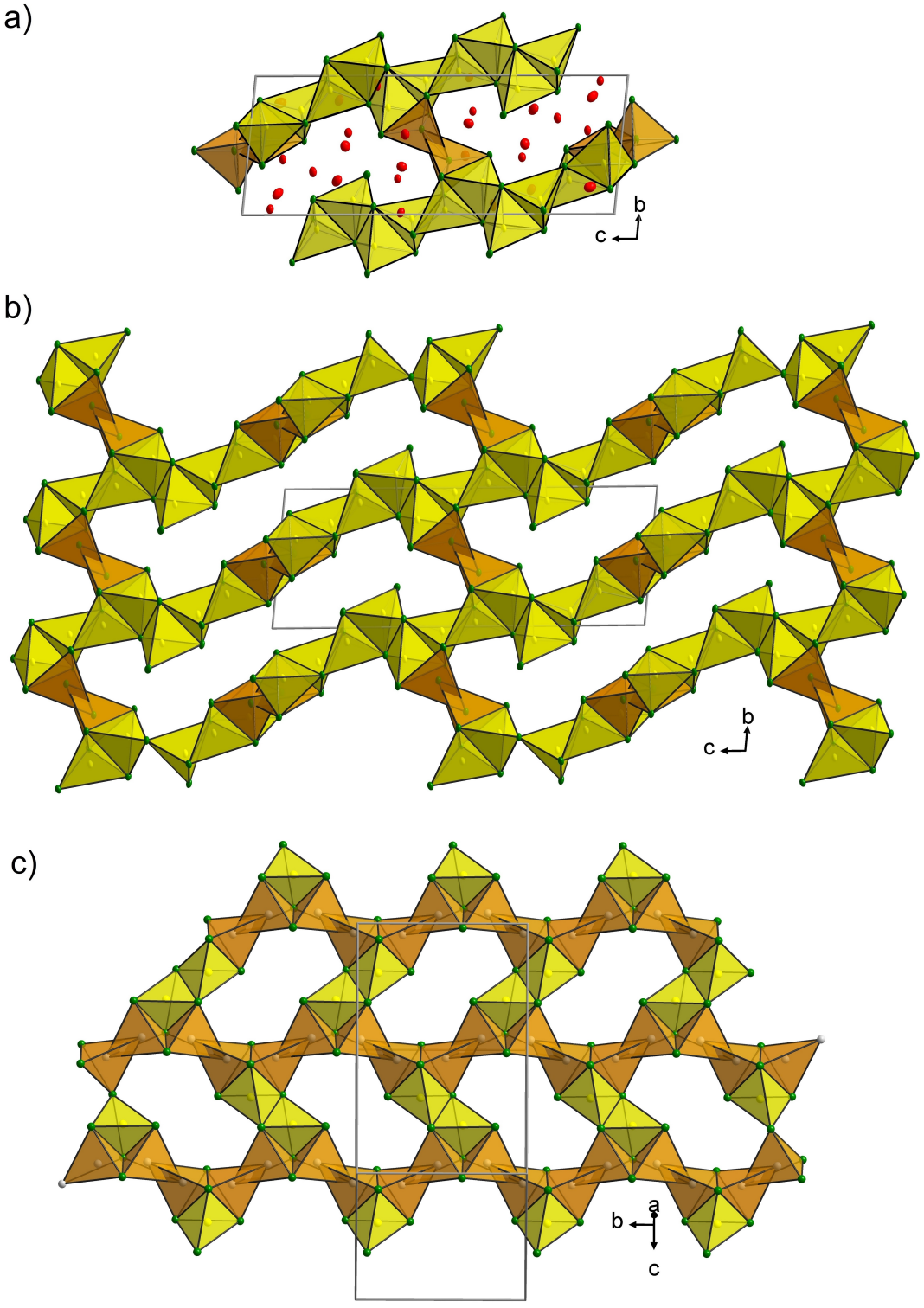

Figure 2. a) The structure of $K_7In_4As_6$, unit cell; b) the stacking of the yellow [In@As_4] and orange [In@As_3In] tetrahedra within one layer along the [100] direction. In atoms are yellow, arsenic atoms green and potassium atoms red, the displacement ellipsoids are drawn at a 90% probability level; c) the structure of $Cs_5In_3As_4$, the layer of the yellow [In@As_4] and orange [In@As_3In] condensed tetrahedra.

Six out of eight In atoms center the As_4 tetrahedra, with In–As distances between 2.592(1) and 2.855(1) Å (Table 2, Figure 3 < figr3). Two other In atoms, In4 and In5, are surrounded by three As atoms, and form In–In bonds ($d_{In4\text{-}In4}$ = 2.833 and $d_{In5\text{-}In5}$ = 2.838 Å, respectively). The ethane analog building unit As_3In–InAs_3 can also be described as two inter-

Table 2. Selected interatomic distances in $K_7In_4As_6$. For details see Table S2 (Supporting Information).

Atom types		Distance range(Å)	Atom types	Distance range(Å)
In	–In	2.834(1)-3.655(1)	K	–In	3.321(2)–4.626(2)
In	–As	2.592(1)-2.855(1)	K	–As	3.214(3)–4.251(3)

penetrating In-centered tetrahedra [In4@As_3In4] and [In5@As_3In5], with the In atoms centering one tetrahedron and forming the vertex of the neighboring tetrahedron (Figure 3e,f). These units are almost perpendicular to the chains of the edge-sharing $InAs_4$ tetrahedra and are linking these chains. The As_3In–$InAs_3$ units or the interpenetrating [In@As_3In] tetrahedra are comparable to those observed in $Cs_5In_3As_4$ (Figure 2c, in orange) with a slightly longer In–In distance of 3.032 Å.[12]

Compound $K_7In_4As_6$ is an electronically balanced phase with the formal fully ionic description $(K^+_{14})(In^{3+})_6(In^{2+})_2(As^{3-})_{12}$, where In^{3+} corresponds to indium atoms coordinated by four As atoms in In@As_4 tetrahedra, and In^{2+} are the In atoms centering the In@As_3In tetrahedra comprising one homoatomic bond. Following Zintl's idea of considering covalent bonds between the atoms of the polyanion and application of the (8-N) rule leads to the formula $(K^+)_{14}[(4b\text{-}In)^-]_8$ $[(3b\text{-}As)^0]_7$ $[(2b\text{-}As)^-]_4[(1b\text{-}As)^{2-}]$ (with nb = n bonded atom), which nicely represents the local bond situation of each atom.

With a slightly lower In to As ratio and a slightly higher K content, K_3InAs_2 contains $InAs_4$ tetrahedra that form a one-dimensional polyanion $^1_\infty[InAs_2]^{3-}$ of exclusively edge-sharing tetrahedra and exclusively $(4b\text{-}In)^-$ and $(2b\text{-}As)^-$ atoms. K_3InAs_2 is isostructural to K_3InP_2,[19] and it crystallizes in the Na_3AlAs_2 structure type.[27] The unit cell is shown in Figure 4. The anionic substructure consists of In-centered As_4 tetrahedra with an In–As distance of 2.719(1) Å (Table 3), which is significantly longer than $d_{In\text{-}P}$ = 2.639 Å in K_3InP_2. The tetrahedra are interconnected through common edges, and the infinite chains propagate along the [001] direction (Figure 4c). Such rods of edge-sharing tetrahedra were first observed as SiS_4 tetrahedra in SiS_2.[28] In K_3InAs_2, the K atoms at two independent Wyckoff positions are separating the rods. K1 is coordinated by four arsenic ($d_{K\text{-}As}$ = 3.304(1)–3.335(1) Å) and two indium atoms ($d_{K\text{-}In}$ = 3.569(1) Å); the K2 atoms are surrounded by four As atoms with an interatomic K–As distance of 3.304(1) Å. K_3InAs_2 is an electronically balanced Zintl phase, which could also be written as $(K^+)_3(In^{3+})_1(As^{3-})_2$.

Table 3. Selected interatomic distances in K_3InAs_2. For details see Table S7 (Supporting Information).

Atom types		Distance range(Å)	Atom types		Distance range(Å)
In	–In	3.468(1)	K	–In	3.569(1)–3.911(1)
In	–As	2.719(1)	K	–As	3.304(1)–4.150(2)

Electronic Structures. LMTO calculations for $K_7In_4As_6$ and K_3InAs_2 confirm semiconducting properties for both phases as expected for Zintl phases with band gaps of 0.5 and 0.6 eV, respectively. The band structure and the total Density of States (DOS) with orbital projected DOS and the separate contributions from the constituting elements are represented in Figures 5 and 6, respectively. The flat bands indicate mainly localized electrons, however, a higher dispersion is observed for $K_7In_4As_6$. The peak at lowest energies in the valence region in the DOS is in the area of −10 eV and is mainly the arsenic s orbitals with small contributions of In and K s orbitals. The region from approx. −6 to 0 eV (E_F) predominantly contains contributions from the p orbitals of As with participation of the s orbitals of potassium and p orbitals of indium. In the conduction band above the Fermi level, the main contributions arise from As and In p orbitals and K s orbitals. Notice that the In states in the region −4 to 0 eV are more prominent for $K_7In_4As_6$ and originate from the In–In interaction. Most interestingly, there are considerable K atom orbital contributions for both compounds, which originate from the interaction with lone pairs of the As atoms.

Summary and Discussion

Zintl phases are good candidates for the formation of compounds with variable band gaps, and many structures have been reported that show a large structural variety of the involved polyanions. It is well established that a higher content of electropositive metals reduces the dimensionality of the polyanions leading to discrete polyanions rather than three-dimensional networks. In the *A–Tr–Pn* system, the alkali metal content influences the dimensionality of the polyanion structure, and in a simple view one might expect that the *Tr* to *Pn* atom ratio within the *A–Tr–Pn* phases influences the structures as well: At a higher *Pn* content the formation of *Pn-Pn* bridges between the tetrahedra might be favored, whereas a higher *Tr* metal content should lead to the formation of *Tr–Tr* bonds.

The average valence electron number of the atoms of the polyanion (valence electron concentration = VEC) allows in general the determination of the bond situation between the atoms of the polyanion. VEC = 4 leads to a three-dimensional network of four-bonded atoms such as in the diamond structure of Tl^- in NaTl. At a VEC of five, three-connected atoms might form a two-dimensional structure such as in the α-As-type layers of Si^- in $CaSi_2$. Nevertheless, also P_4-analogous clusters might result, as observed in KSi (= K_4Si_4).

The influence of the cation becomes obvious in K_3InAs_2 that has the same electron count as Na_3InAs_2 (VEC_{anion} = 5.3), but shows a one-dimensional structure in contrast to the 3D structure of the latter. The title compound $K_7In_4As_6$ contains the third example of polyanions with the same ratio In : As = 2 : 3. However the three compounds, $K_2In_2As_3$, $K_3In_2As_3$ and $K_7In_4As_6$ (= $K_{3.5}In_2As_3$) differ slightly in their VECs that are 4.6, 4.8 and 4.9, respectively (Table 4). The first two examples have a 2D structure, whereas the latter even though having a VEC close to five forms a 3D structure (Figures 1 and S1, Supporting

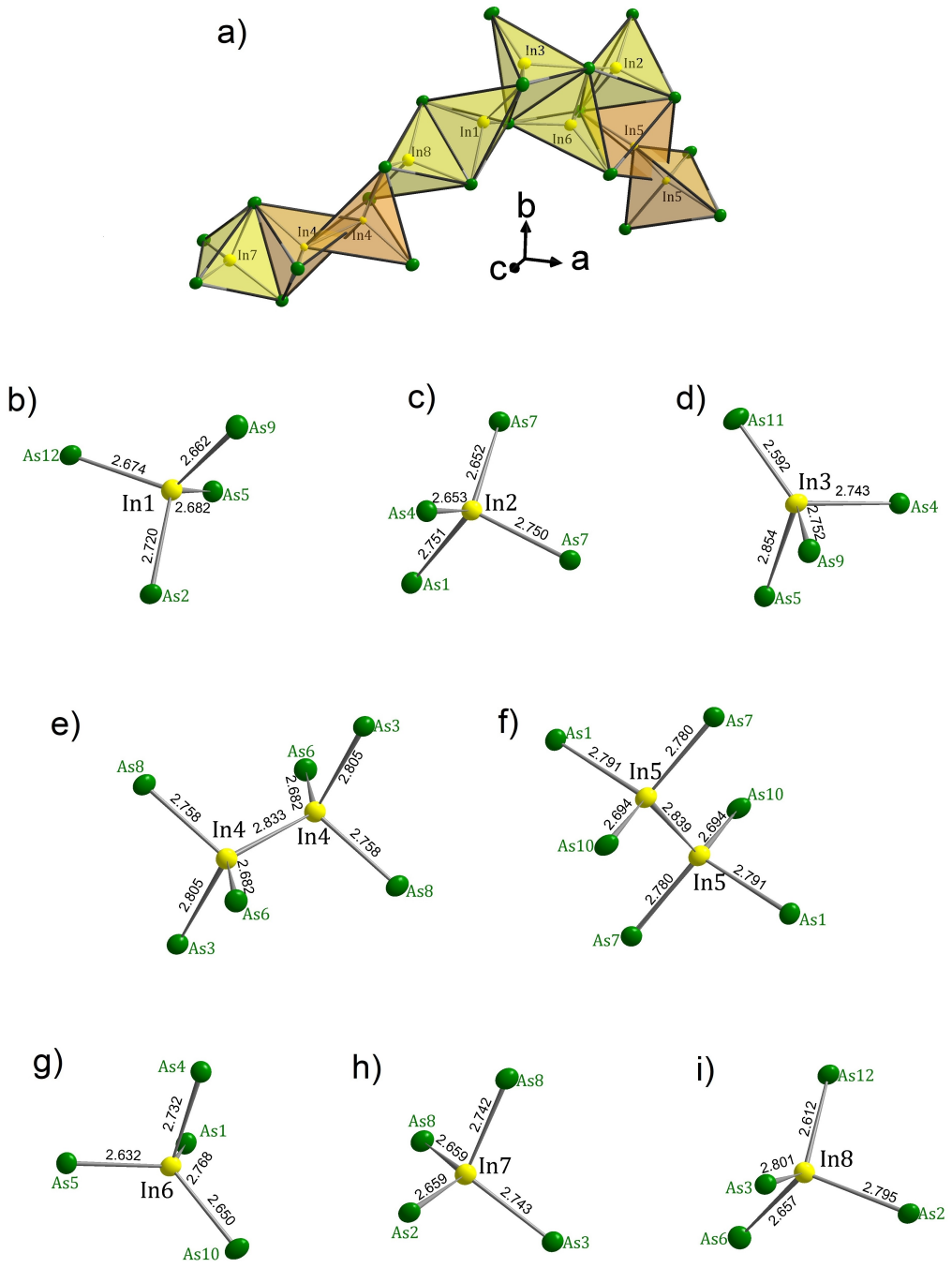

Figure 3. A structural fragment of $K_7In_4As_6$ (a) and the environment of the In-atoms: indium atoms (In1-In3, In6-In7) centering As_4 tetrahedra (b–d, g–k) and intercalated tetrahedra around In4 (d) and In5 (e) atoms.

Information). The lack of a simple trend originates from the large variety of the bonding modes of the As atoms that reach from $(3b\text{-}As)^0$ to $(2b\text{-}As)^-$ and $(1b\text{-}As)^{2-}$. All three modes are observed in the phase $K_7In_4As_6$, and according to the 8-N rule it can be described as $(K^+)_{14}[(4b\text{-}In)^-]_8[(3b\text{-}As)^0]_7[(2b\text{-}As)^-]_4[(1b\text{-}As)^{2-}]$. In addition, the formation of In–In bonds is observed. With a lower VEC of the anion the number of higher charged As atoms decreases according to $(K^+)_3[(4b\text{-}In)^-]_2[(3b\text{-}As)^0]_2[(2b\text{-}As)^-]$ and $(K^+)_2[(4b\text{-}In)^-]_2[(3b\text{-}As)^0]_3$ for $K_3In_2As_3$ and $K_2In_2As_3$, respectively, with the latter also comprising As–As bonds.

In $Cs_5In_3As_4$ with VEC = 4.9 even three-fold bonded In atoms are present, that thus have a formal charge of −2, and finally in A_6InAs_3 (A = K, Cs) with the highest VEC = 6 discrete ionic units appear that in analogy to the carbonate anion comprise an electron sextet at the In atom or an In–As double bond.

The examples show that a large variety of polyanions can arise by combination of only two elements depending on the

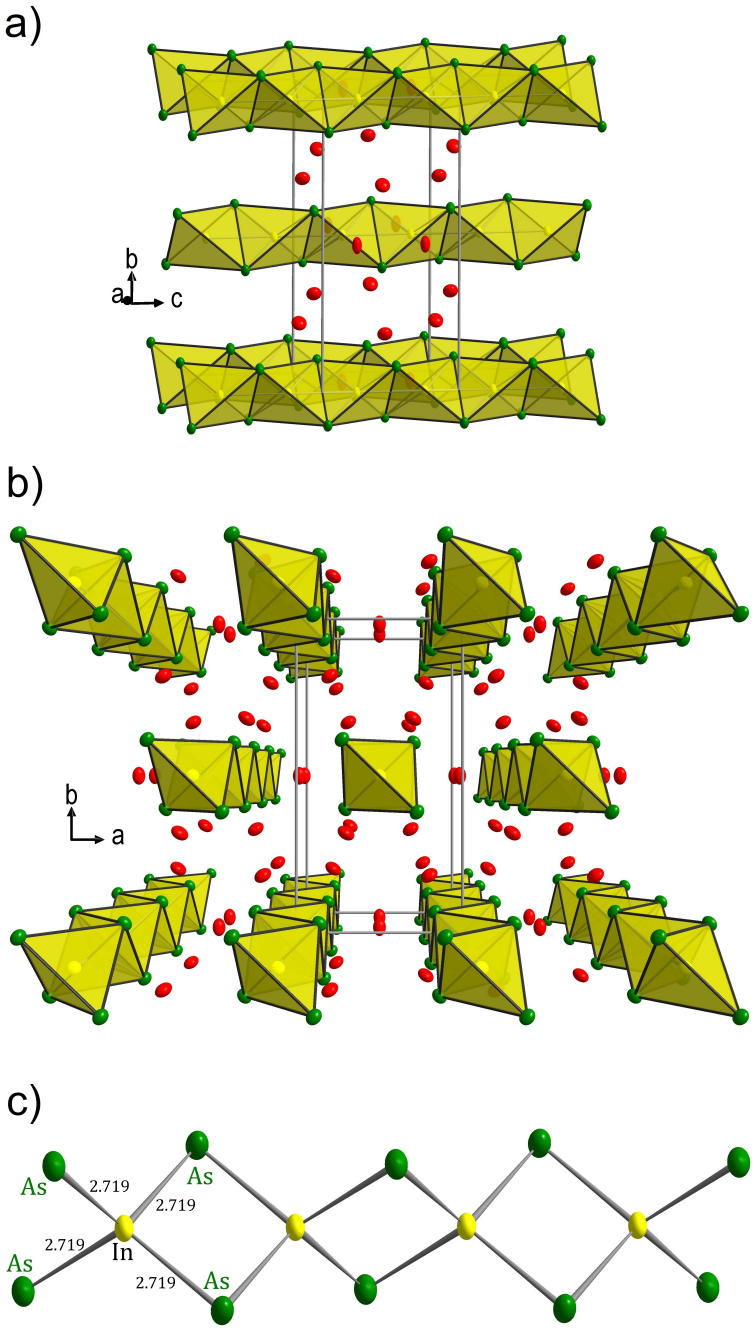

Figure 4. a) and b) two viewing directions of the extended unit cell of K_3InAs_2; c) the polyanion $^1_\infty[InAs_2]^{3-}$ along [001]. In, As and K atoms are shown with yellow, green and red color, respectively. In-centered As_4 tetrahedra are highlighted with yellow-colored faces. All displacement ellipsoids are drawn at a 90% probability level.

ratio of the two components and the size of the alkali metal atom. The possible formation of homoatomic beside the heteroatomic bonds allows for an even larger number of possible structures. Thus, the prediction of new structures based on the Zintl concept is difficult. Since Zintl phases with their immense scope of band gap tuning are increasingly important, the results here consequently demand for explorative syntheses.

Acknowledgements

The authors thank for funding this work in the scope of the project "Solar Technologies go Hybrid" supported by the Bavarian State Ministry of Science and the Arts. Open Access funding enabled and organized by Projekt DEAL.

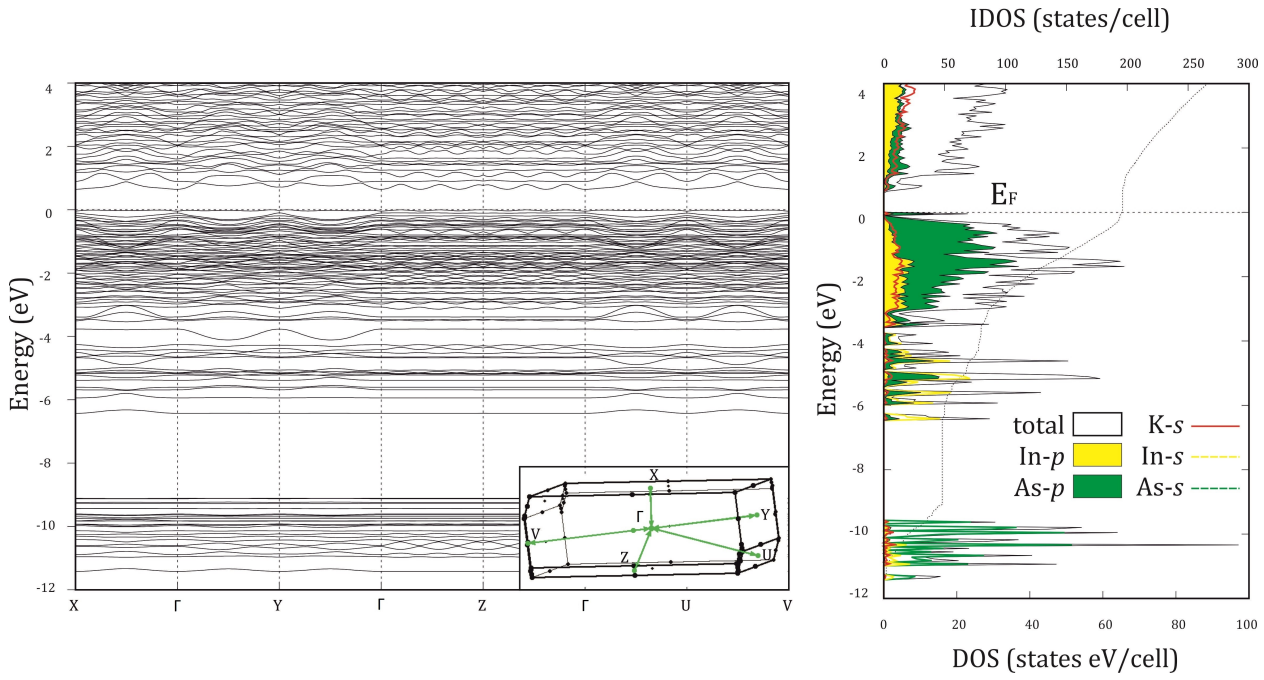

Figure 5. The band structure and the total Density of States (DOS) with orbital-projected DOS calculated for $K_7In_4As_6$.

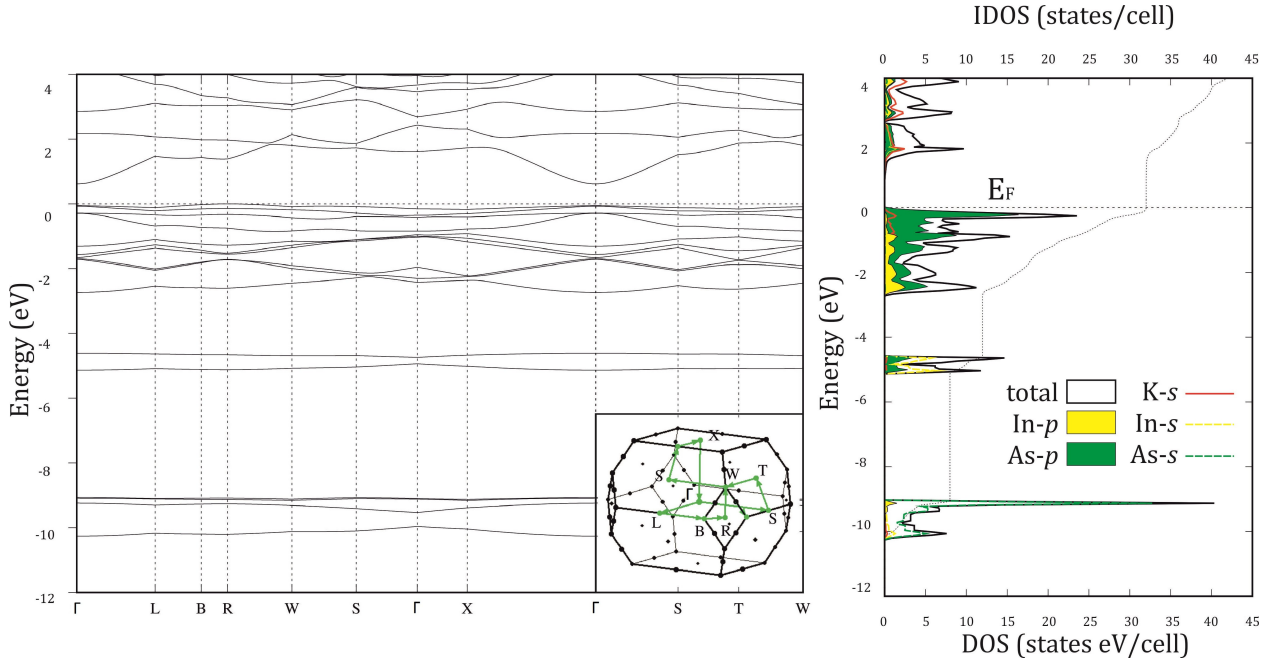

Figure 6. The band structures and the total Density of States (DOS) with orbital-projected DOS calculated for K_3InAs_2.

Conflict of Interest

The authors declare no conflict of interest.

Data Availability Statement

The data that support the findings of this study are available in the supplementary material of this article.

Table 4. Known alkali metal compounds with polyanions composed of In and As atoms.

formula	polyanion dimension[1])	In : As ratio	$VEC_{poly\text{-}anion}$ [2])	notation according to the 8-N rule [3])
$K_2In_2As_3$	2D (As–As)	2 : 3 = 0.66	4.6	$(K^+)_8[(4b\text{-}In)^{1-}]_8\,[(3b\text{-}As)^0]_{12}$
$K_3In_2As_3$	2D	2 : 3	4.8	$(K^+)_{12}[(4b\text{-}In)^{1-}]_8[(3b\text{-}As)^0]_8\,[(2b\text{-}As)^-]_4$
$K_7In_4As_6$	3D (In–In)	2 : 3	4.9	$(K^+)_{14}[(4b\text{-}In)^{1-}]_8\,[(3b\text{-}As)^0]_7[(2b\text{-}As)^-]_4[(1b\text{-}As)^{2-}]$
$Cs_5In_3As_4$	2D (In–In)	3 : 4 = 0.75	4.9	$(Cs^+)_{10}[(4b\text{-}In)^{1-}]_5[(3b\text{-}In)^{2-}][(3b\text{-}As)^0]_5[(2b\text{-}As)^{1-}]_3$
K_3InAs_2	1D	1 : 2 = 0.5	5.3	$(K^+)_{12}[(4b\text{-}In)^{1-}]_4\,[(2b\text{-}As)^-]_8$
Na_3InAs_2	3D	1 : 2 = 0.5	5.3	$(Na^+)_{12}[(4b\text{-}In)^{1-}]_4\,[(2b\text{-}As)^-]_8$
A_6InAs_3 (A = K, Cs)	0D	1 : 3 = 0.3	6	$(K^+)_6[(3b\text{-}In)^0][(1b\text{-}As)^{2-}]_3$

[1]) In addition, the appearance of homoatomic In–In or As–As bond formation is listed. D = dimensional. [2]) VEC_{anion} is calculated adding the electrons of the atoms In and As (3 and 5, respectively) and adding the charges according to the number of alkali metal atoms. The total number of electrons is divided by the sum of In and As atoms. [3]) For the reason of comparison, a multiple of the formula is used.

[1] a) V. G. Tissen, V. F. Degtyareva, M. V. Nefedova, E. G. Ponyatovskii, W. B. Holzapfel, *J. Phys. Condens. Matter* **1998**, *10*, 7303; b) C.-M. Lin, S.-C. Lin, Y.-C. Tseng, T. Huang, H.-H. Kung, Y.-C. Chuang, Y.-F. Liao, B.-R. Wu, S.-R. Jian, J.-Y. Juang, *J. Phys. Chem. Solids* **2022**, *161*, 110487.
[2] S. Kasap, P. Capper, *Springer Handbook of Electronic and Photonic Materials*, in Springer, **2007**.
[3] a) A. B. Childs, S. Baranets, S. Bobev, *J. Solid State Chem.* **2019**, *278*, 120889; b) K. Rajput, S. Baranets, S. Bobev, *Chem. Mater.* **2020**, *32*, 9616–9626; c) J. Mathieu, R. Achey, J.-H. Park, K. M. Purcell, S. W. Tozer, S. E. Latturner, *Chem. Mater.* **2008**, *20*, 5675–5681; d) G. Cordier, H. Schaefer, M. Stelter, *Z. Naturforsch. B* **1986**, *41*, 1416–1419; e) F. Gascoin, S. C. Sevov, *Inorg. Chem.* **2002**, *41*, 2292–2295; f) W. Peng, S. Baranets, S. Bobev, *Crystals* **2022**, *12*, 1467; g) S. S. Stoyko, L. H. Voss, H. He, S. Bobev, *Crystals* **2015**, *5*, 433–446; h) V. Weippert, A. Haffner, A. Stamatopoulos, D. Johrendt, *J. Am. Chem. Soc.* **2019**, *141*, 11245–11252.
[4] a) W. Blase, G. Cordier, M. Somer, *Z. Kristallogr.* **1991**, *195*, 117–118; b) W. Blase, G. Cordier, M. Somer, *Z. Kristallogr.* **1993**, *206*, 141–142.
[5] M. Somer, D. Thiery, M. Hartweg, L. Walz, K. Peters, H. G. v. Schnering, *Z. Kristallogr.* **1990**, *193*, 287–288.
[6] G. Cordier, H. Ochmann, *Z. Naturforsch. B* **1990**, *45*, 277–282.
[7] G. Cordier, H. Ochmann, *Z. Kristallogr.* **1991**, *195*, 111–112.
[8] a) T. M. F. Restle, C. Sedlmeier, H. Kirchhain, W. Klein, G. Raudaschl-Sieber, V. L. Deringer, L. van Wüllen, H. A. Gasteiger, T. F. Fässler, *Angew. Chem. Int. Ed.* **2020**, *59*, 5665–5674; b) T. M. F. Restle, S. Strangmüller, V. Baran, A. Senyshyn, H. Kirchhain, W. Klein, S. Merk, D. Müller, T. Kutsch, L. van Wüllen, T. F. Fässler, *Adv. Funct. Mater.* **2022**, *32*, 2112377; c) M. Somer, W. Carrillo-Cabrera, J. Nuss, K. Peters, H. G. von Schnering, G. Cordier, *Z. Kristallogr.* **1996**, *211*, 550; d) M. Somer, W. Carrillo-Cabrera, J. Nuss, K. Peters, H. G. von Schnering, G. Cordier, *Z. Kristallogr.* **1996**, *211*, 479–480; e) G. Cordier, H. Schäfer, M. Stelter, *Z. Naturforsch. B* **1985**, *40*, 868–871; f) S. L. Brock, L. J. Weston, M. M. Olmstead, S. M. Kauzlarich, *J. Solid State Chem.* **1993**, *107*, 513–523; g) W. Carrillo-Cabrera, M. Somer, K. Peters, H. G. von Schnering, *Chem. Ber.* **1996**, *129*, 1015–1023; h) G. Cordier, H. Schäfer, M. Stelter, *Z. Anorg. Allg. Chem.* **1984**, *519*, 183–188.
[9] M. Boyko, V. Hlukhyy, T. F. Fässler, *Z. Anorg. Allg. Chem.* **2020**, *646*, 659–664.
[10] F. A. Cotton, G. Wilkinson, P. L. Gaus, *Basic Inorganic Chemistry*, 2nd. Ed. ed., John Wiley and Sons, New York, **1987**, p. 332.
[11] Inorganic Crystal Structure Database, PC Version Release 2023/1 ed., Fachinformationszentrum Karlsruhe, Germany, **2023**.
[12] F. Gascoin, S. C. Sevov, *Inorg. Chem.* **2001**, *40*, 6254–6257.
[13] G. Cordier, H. Ochmann, *Z. Kristallogr.* **1991**, *197*, 293–294.
[14] G. Cordier, H. Ochmann, *Z. Kristallogr.* **1991**, *197*, 295–296.
[15] G. Cordier, H. Ochmann, *Z. Kristallogr.* **1991**, *195*, 105–106.
[16] STOE, Version 3.0.2.1 ed., STOE & Cie GmbH, Darmstadt **2011**.
[17] a) G. M. Sheldrick, University of Goettingen, Goettingen, Germany, **2014**; b) G. M. Sheldrick, University of Goettingen, Goettingen, Germany, **2014**.
[18] J. Koziskova, F. Hahn, J. Richter, J. Kožíšek, *Acta Chim. Slov.* **2016**, *9*, 136–140.
[19] W. Blase, G. Cordier, *Z. Kristallogr.* **1991**, *195*, 109–110.
[20] P. Villars, in *SpringerMaterials (online database)*, Springer, Heidelberg (ed.), **2023**.
[21] M. v. Schilfgarde, T. A. Paxton, O. Jepsen, O. K. Andersen, G. Krier, Version 4.7 ed., Max-Planck-Institut für Festkörperforschung Stuttgart (Germany), **1998**.
[22] O. Jepsen, O. K. Andersen, *Z. Phys. B* **1995**, *97*, 35–47.
[23] W. R. L. Lambrecht, O. K. Andersen, *Phys. Rev. B* **1986**, *34*, 2439–2449.
[24] W. Setyawan, S. Curtarolo, *Comput. Mater. Sci.* **2010**, *49*, 299–312.
[25] M. I. Aroyo, D. Orobengoa, G. de la Flor, E. S. Tasci, J. M. Perez-Mato, H. Wondratschek, *Acta Crystallogr. Sect. A* **2014**, *70*, 126–137.
[26] S. Bobev, S. C. Sevov, *Inorg. Chem.* **1999**, *38*, 2672–2675.
[27] G. Cordier, H. Ochmann, *Z. Naturforsch.* **1988**, *43b*, 1538–1540.
[28] J. Peters, B. Krebs, *Acta Crystallogr. Sect. B* **1982**, *38*, 1270–1272.

Manuscript received: July 25, 2023
Revised manuscript received: September 11, 2023
Accepted manuscript online: September 14, 2023

